Journal Pre-proof

High strength PLGA/Hydroxyapatite composites with tunable surface structure using PLGA direct grafting method for orthopedic implants

Ji-Won Park, Jin-Uk Hwang, Jong-Ho Back, Seong-Wook Jang, Hyun-Joong Kim, Pan-Seok Kim, Seunghan Shin, Taejin Kim

PII: S1359-8368(19)32946-4

DOI: https://doi.org/10.1016/j.compositesb.2019.107449

Reference: JCOMB 107449

To appear in: *Composites Part B*

Received Date: 24 June 2019

Revised Date: 8 September 2019

Accepted Date: 14 September 2019

Please cite this article as: Park J-W, Hwang J-U, Back J-H, Jang S-W, Kim H-J, Kim P-S, Shin S, Kim T, High strength PLGA/Hydroxyapatite composites with tunable surface structure using PLGA direct grafting method for orthopedic implants, *Composites Part B* (2019), doi: https://doi.org/10.1016/j.compositesb.2019.107449.

High strength PLGA/Hydroxyapatite composites with tunable surface structure using PLGA direct grafting method for orthopedic implants

Ji-Won Park[1,2], Jin-Uk Hwang[1], Jong-Ho Back[1], Seong-Wook Jang[2], Hyun-Joong Kim[1,2†], Pan-Seok Kim[3], Seunghan Shin[4] and Taejin Kim[1,5]

[1] Laboratory of Adhesion and Bio-Composites, Program in Environmental Materials Science, Seoul National University, Seoul 151-921, Republic of Korea

[2] Research Institute of Agriculture and Life Sciences, College of Agriculture and Life Sciences, Seoul National University, Seoul 151-921, Republic of Korea

[3] ARC Korea Co., Ltd. 14, Nonhyeon-ro 31gil Seocho-gu, Seoul 137-886, Republic of Korea

[4] Green Process R&D Department, Korea Institute of Industrial Technology, Cheonan-si, Chungnam 31056, Republic of Korea

[5] Materials Science and Chemical Engineering Department, Stony Brook University, NY, United States

Graphical Abstract

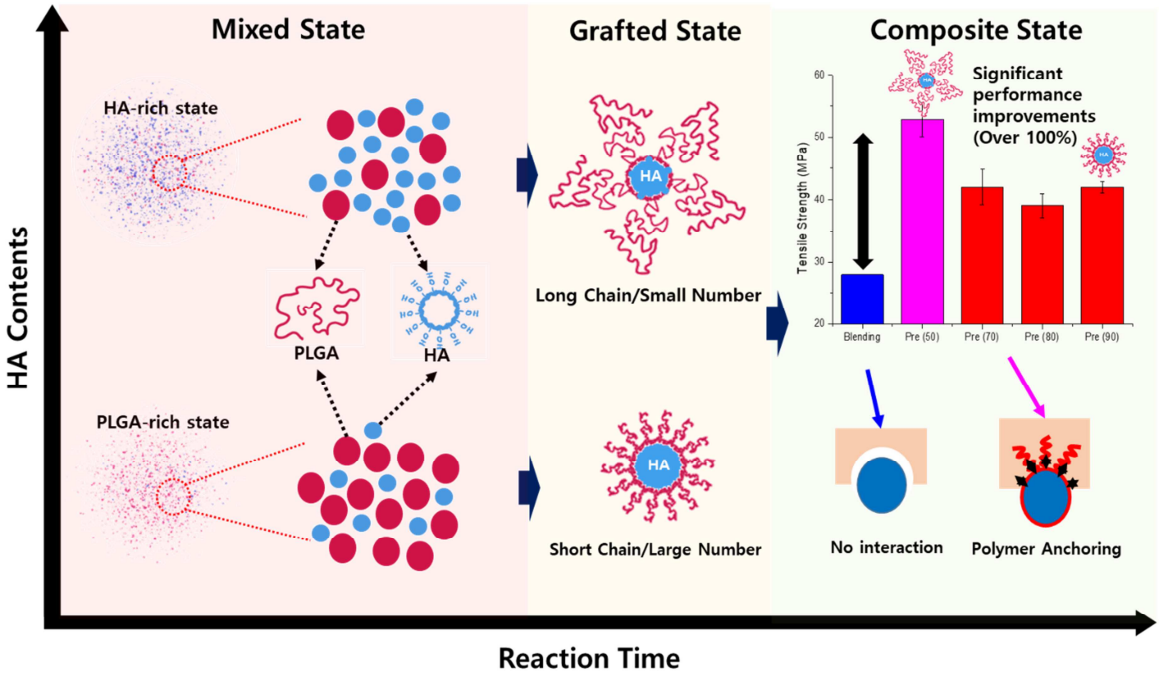

ABSTRACT

Poly (Lactic-co-Glycolic Acid) (PLGA) based bio-composites for orthopedic implants are becoming more important as surgical techniques develop. Enhancers such as hydroxyapatite (HA) are used to enhance the biocompatibility and bone formation. Studies on HA surface treatment have been proposed to enhance the bonding force between particles HA and PLGA. Conventional monomer-based grafting techniques have limitations in copolymer grafting and improving mechanical strength of composites. In this study, PLGA can be directly grafted to HA surface in polymer state using melt grafting with transesterification. With this method, the grafting efficiency of PLGA is improved compared to previous studies. The grafting efficiency of PLGA was analyzed and the structure at the surface was confirmed. It was confirmed that a polymer having a large molecular weight can be grafted on the HA surface when PLGA is in an abundant state by indirectly analyzing the size of the grafting polymer through molecular weight evaluation. A composite materials using PLGA-g-HA prepared under optimized conditions have tensile strengths increased by more than doubled compared with a n-HA blended composite. The direct grafting technique of polymer was found to be effective in forming the anchoring structure between HA particles and PLGA.

KEYWORDS: Poly (Lactic-co-Glycolic Acid), Hydroxyapatite, Medical Composites, Surface treatment, Direct Polymer Grafting, Melt grafting with Transesterification, Interface, Characterization

1. INTRODUCTION

Many procedures have been performed to fix broken bones or to connect torn ligaments or tendons between joints. These surgeries are often required due to the extension of the typical life span caused by the development of medical technologies and the expansion of leisure activities due to social and cultural changes. The average life span is expected to steadily grow as society continues to change[1-3]. A rotator cuff tear is the rupture of a tendon to the essential muscle in the shoulder joint and is the most common degenerative problem in adults. The number of patients requiring rotator cuff repair is rapidly increasing due to aging and improvement in the quality of life, and the social costs associated with the treatment and its aftereffects are increasing. In the United States, more than 300,000 surgeries are performed each year[4, 5]

Conventionally, the methods for fixing a broken bone or repairing a ligament or tendon requires the use of various surgical instruments, which complicates the operation and prolongs the operation time. Therefore, the development of a ligament fixation screw that is easy to operate, economical and not a physical burden to doctors and patients is required. The screw used for such a surgery is called a bio-screw.[6, 7] Recently, an arthroscopic technique has begun to be used. In the arthroscopic technique, a small tube is inserted at the surgical site, and surgery is performed through this tube. Therefore, the strength of the screw used to make the repair is very important because the diameter of the tube that the screw is inserted through is small.[8-10]

Bio-screws prepared using biodegradable polymers effectively overcome the disadvantages of metal-based bio-screws. Since the screw decomposes in the body and does not interfere during imaging, it can improve the outcome of surgery. The biodegradable bio-screws, which mainly used poly (lactic acid) (PLA), Poly(L-lactic acid) (PLLA) and poly(lactic-co-glycolic acid) (PLGA). However, pure biodegradable polymer screws have a disadvantage in that they are not

only slow to degrade but also do not accelerate the growth of bone tissue because these polymers itself is not compatible with the bone tissue.[11, 12]. To overcome these disadvantages, inorganic ceramics, called enhancers, such as beta-tricalcium phosphate (b-TCP) and hydroxyapatite (HA) are used together with polymers. These enhancers have components that are similar to bone and thus accelerate bone growth and minimize the side effects in the screw space. Biomaterials are all recognized as foreign substances by living organisms, so foreign substances are highly reactive and become breeding grounds for bacteria and are thus likely to cause infection. By modifying the surface of such an artificial material with a biomaterial capable of inducing cell growth, the existing tissue growth and compatibility can be improved while minimizing the reactivity of the foreign matter and protecting against infection.[13, 14]

Materials such as enhancers are poorly compatible with polymer matrices and therefore decrease the strength of the bio-screw. Traditionally, composite materials utilizing both inorganic and organic materials have been studied in various ways. The most important issue in this process is to find ways to enhance the compatibility with organic materials by treating inorganic surfaces [15, 16]. In the past, research has been focused on attaching monomers of polymers to inorganic surfaces, but recently, eco-friendly and human-friendly technologies are being introduced using biomimetic technologies. Surface modification studies using mussel or lignocellulose materials are a prime example [15, 17, 18]. This technique has yielded effective results for selectively controlling the surface of the inorganics. However, these technologies have limitations for use in the technology immediately available in the medical field. Previous studies have applied compatibilizers in composite materials by attaching monomers to the surface of the ceramic and growing polymers from the adhered monomers [19-21]. In particular, various techniques for polymerizing PLA on the surface have been proposed. These studies were

conducted to prepare PLA-g-HA through graft polymerization from the HA surface and to enhance the binding force with PLGA or PLA [22-24]. Previous monomer-based grafting techniques have limitations in copolymer grafting. The methods cannot graft copolymer at an exact ratio. In addition, this approach could not be used to grafting polymers of sufficient length on the surface, resulting in improved compatibility, while not having a significant effect on improving mechanical strength [25, 26]. One of the reasons PLGA is used in the medical field is to reduce crystallinity and enhance biodegradability through the ratio of L and G. And, the previous studies have focused on the analysis of grafting weight traction rather than the structure of grafting [27, 28].

In this study, PLGA-grafted HA (PLGA-g-HA) was prepared by direct grafting PLGA molecules on the surface of HA using the melt reaction with transesterification. We analyzed the changes in PLGA-g-HA as a function of the ratio of the materials and the environmental conditions of the reaction process and examined the possibility of using the composite materials. FT-IR, NMR, TGA, FE-SEM, XRD, DSC, and GPC were used in order to observe the change of surface state according to process conditions. Finally, composite materials were prepared using PLGA-g-HA, and their mechanical properties were evaluated to confirm the effect of direct grafting.

2. EXPERIMENTAL

2.1. Materials

PLGA exhibits a variety of properties depending on the ratio of lactic acid to glycolic acid. For example, the crystallinity and decomposition characteristics are determined by the ratio of the two materials. PLGA decomposes most rapidly when the ratio of lactic acid to glycolic acid is

50:50. However, a bio-screw should decompose slowly over 6 to 24 months in the body, so PLGA with an appropriate ratio should be selected and used.[28, 29] In the case of bio-screws, the ratio of lactic acid should be large because the screw must possess rigid properties. In this study, PLGA (Corbion Purac, Netherlands) with a lactic acid to glycolic acid ratio of 82:18 was used. To maximize the dispersibility, a solvent dispersion technique was used. The solubility of PLGA varies with the ratio of the two materials and is excellent in chloroform when the ratio of lactic acid is large.[30] In this study, chloroform of 99.8% purity (Samchun Pure Chemical, Republic of Korea) was used without purification, and HA (Sigma-Aldrich, USA) was used as the enhancer.

2.2. Grafting Reaction of PLGA on the Surface of HA

Figure 1 shows the whole process for making PLGA-g-HA. PLGA was dissolved in chloroform under magnetic stirring at 50 □ for 6 h. After the PLGA pellets dissolved, HA was added to the solution and blended by magnetic stirring at 50 □ for 6 h. To uniformly disperse HA with the polymer chains, the PLGA/HA suspension was sonicated at room temperature for 3 hours and then dried at 50 □ for 6 hours to remove the chloroform. The dried sample was transferred to a 200□ oven to induce the reaction between PLGA and HA. The reaction proceeded for 3 to 120 minutes. After reaction, the mixture was transferred to a conical tube and dispersed in chloroform by sonication at room temperature for 3 hours, and then the supernatant and sediment were separated by centrifugation at 3,000 rpm for 10 min. The molecular weight of the dissolved PLGA was measured using the solution obtained from the first purification step. The first purified product was resuspended in chloroform and subjected to ultra-sonication at room temperature for 3 hours. The centrifugation procedure was carried out again using the

solution from the first purified product. The particles obtained through centrifugation were washed and dried at 50 ° C for 24 hours to obtain the final sample.

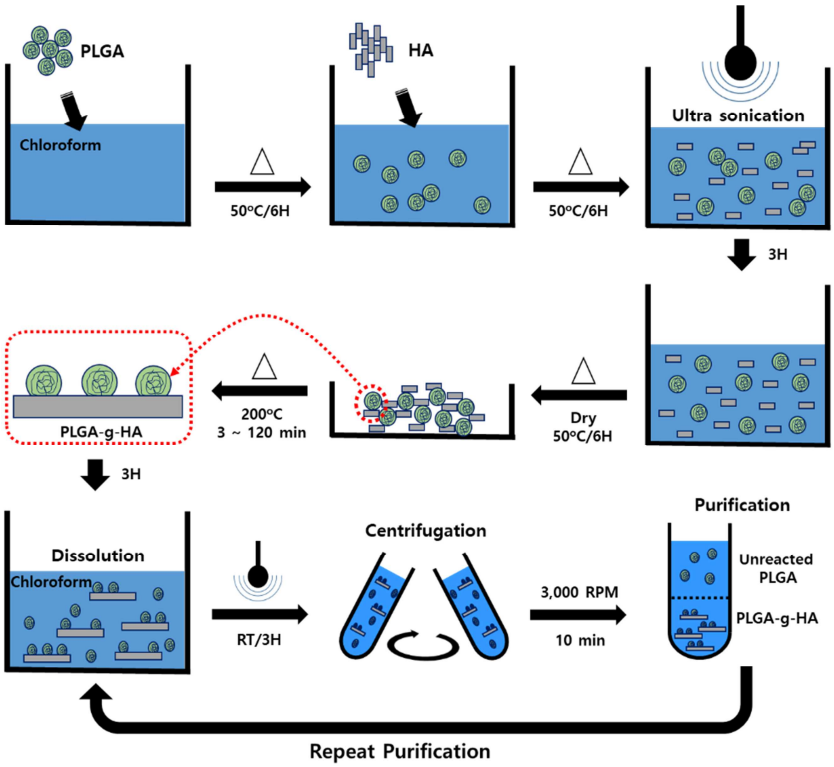

Figure 1. Process for preparing PLGA-g-HA.

2.3. Characterization of the PLGA-g-HA Particles

2.3.1. Fourier Transform Infrared (FT-IR) Spectroscopy

Infrared spectra were obtained using an FT-IR spectrometer (FT/IR-6100, JASCO, MD 21601 USA) equipped with a Mylar beam splitter and an attenuated total reflectance (ATR) accessory composed of a zinc selenide (ZnSe) crystal (refractive index = 2.4) with a 45° angle of incidence. The spectra were collected from 4000 cm^{-1} to 400 cm^{-1} for 32 scans with a resolution of 4 cm^{-1}. All spectra were corrected through CO_2 reduction, H_2O reduction, noise elimination and baseline correction.

2.3.2. Solid-State Nuclear Magnetic Resonance (NMR) Spectroscopy

Solid-state ^{1}H NMR spectra were obtained with a 500 MHz solid NMR system (AVANCE II 500, BRUKER, MA 01821, USA) with the cross polarization (CP) and magic-angle spinning (MAS) technique. The spectrometer was operated at the Larmor frequency of 500.13 MHz in a 4 mm CP/MAS probe head. The spinning frequency of MAS was 10 kHz, and the 90° pulse length was 3.3 µs. A total of 32 scans were recorded with a recycle delay of 3 s. For the solid-state ^{31}P NMR spectra, the spectrometer was operated at the Larmor frequency of 202.45 MHz in a 4 mm CP/MAS probe head. The spinning frequency of MAS was 10 kHz, and the 90° pulse length was 2.0 µs. A total of 256 scans were recorded with a recycle delay of 1 s.

2.3.3. Thermogravimetric Analysis (TGA)

TGA (TGA 4000, PerkinElmer, MA 02451, USA) was used to determine the occurrence of the grafting reaction and to qualitatively measure the weight of the grafted PLGA on the HA surface. A 15 mg to 20 mg portion of the sample was loaded in the chamber, and a 20.0 ml/min flow of nitrogen gas was used as the purge gas. After holding for 1 minute at 30 □, the temperature was scanned from 30 □ to 700 □ at a heating rate of 10 □/min. The TGA furnace was cooled by a circulating water device.

2.3.4. Gel Permeation Chromatography (GPC)

The oven-dried supernatant from the first separation was dissolved in tetrahydrofuran (THF) and sonicated at room temperature for 30 min. The concentration of the solution was 1.5 wt %. Molecular weights were measured using a GPC instrument (YL9100 GPC System, YoungLin Instruments, Anyang-si 14042, Republic of Korea) equipped with a refractive index (RI) detector (YL9170, YoungLin Instruments). The GPC columns were eluted with THF at 35 □ and a flow rate of 1 ml/min. The number-average (M_n) and weight-average (M_w) molecular weights were calculated using a calibration curve made from polystyrene standards.

2.3.5. Scanning Electron Microscopy (SEM)

SEM was conducted using a SUPRA 55VP FESEM system (Carl Zeiss, German) to characterize the morphology of the PLGA-g-HA particles. After being oven-dried at 50 □ for 24 h, the particles were fixed on a cupreous stub with carbon tape and coated with a thin layer of platinum at a sputter current of 30 mA for 140 sec. Imaging was performed at an accelerating voltage of 2 kV and a working distance of 3.6 mm to capture SEM images of pure HA and PLGA-g-HA.

2.3.6. X-ray Diffraction (XRD)

XRD patterns were obtained using an Ultima III Powder diffractometer (Rigaku, Japan) to determine the crystalline structure of the PLGA-g-HA powders. The powders were thoroughly compressed on the sample holder. The diffractometer was operated with Cu Kα radiation (λ = 1.54 Å) at 40 kV and 30 mA from a fixed graphite monochromator. The scanning range of the Bragg angle (2θ) was from 2° to 60° at a rate of 2°/min with a step size of 0.02°. The crystallite size (D) of the HA and PLGA-g-HA powders was determined using the diffraction peak for the (002) plane and Scherrer's equation.

2.3.7. Differential Scanning Calorimetry (DSC)

DSC was performed using a DSC Q200 system (TA Instruments, USA) with an RCS 90 refrigerator cooler to determine the glass transition (Tg), crystallization (Tc), and melting temperatures (Tm) of PLGA-g-HA. Approximately 5 mg of the sample was loaded in a Tzero aluminum pan, and a 50.0 ml/min flow of high-purity nitrogen gas was used as the purge gas. The samples were first scanned from 30 □ to 200 □ at a heating rate of 10 □/min to erase any previous thermal history. After being rapidly quenched to -50 □, the samples were scanned again

from -50 □ to 200 □ at a heating rate of 5 □/min. The degree of crystallinity (Xc) was calculated using the following equation:

2.4. Preparation of the PLGA/PLGA-g-HA Composites

A mass of PLGA-g-HA was ground into powder, and PLGA pellets were milled in a mortar. PLGA/PLGA-g-HA composites were prepared through three different methods of blending before injection molding. All composites were prepared with a PLGA to PLGA-g-HA ratio of 70:30 by weight. The first method was extrusion using a twin-screw compounding extruder (BA-7, L/D = 40/7, Bautek, Republic of Korea). In the preparation method, PLGA and PLGA-g-HA were dispersed in chloroform under magnetic stirring at 50 □ for 6 h. The suspension was dried at 50 □ for 24 h to remove the residual chloroform, and then the product was cut into small pieces. For the control group, a 70:30 weight ratio of PLGA to HA was heat-treated at 200 □ for 3 min to anneal the sample.

2.5. Characterization of the PLGA/PLGA-g-HA Composites

2.5.1. Tensile Strength Test

Indicators of mechanical strength of bio-screws are pull-out strength and torsional strength. Both tests are a measure of the performance of bios-crews immobilized on bones, and their performance varies greatly depending on screw designs and bone conditions, making it difficult to quantitatively compare them. Among the mechanical strengths of the material, it was confirmed through the clinical test that the mechanical strength of the bio-screw and the tensile strength of the material. In this study, the tensile strength was evaluated to predict the strength of the bio-screw.

Dog bone-shaped tensile strength specimens were prepared according to ASTM D638 (Type V). The tensile strength test was carried out using an AllroundLine Z010 Universal Testing

Machine (UTM, Zwick, German) at a crosshead speed of 10 mm/min at room temperature. A 200-kN load cell with a pincer 8222 grip using an extensometer was used for the test. The grip-to-grip separation was 20 mm, and the pre-load was 1 N at a rate of 5 mm/min. At least five specimens were tested, and the tensile strength, modulus and elongation were obtained by averaging the data of five specimens.

2.5.2. Dynamic Mechanical Analysis (DMA)

Rectangular DMA specimens were prepared with dimensions of 60 mm × 12 mm × 3 mm, and DMA was carried out using a DMA Q800 system (TA Instruments, USA). The measurements were performed under DMA multi-frequency-strain mode at a fixed frequency of 1 Hz with a dual cantilever clamp having a span length of 35 mm while purging with 50 ml/min of liquid nitrogen. The oscillating amplitude was 40 µm. The temperature scanning range was from 30 □ to 140 □ at the heating rate of 3 □/min. The storage modulus, loss modulus, and tan delta (damping factor) were measured.

3. RESULTS & DISCUSSION

The PLGA present on the HA surface must be directly bonded to the HA for composite stability. In the surface treatment process, PLGA is physically covered with HA surface and chemically combined with HA. Chemical bonding is important for stability in the process of making composites. Therefore, it is very important to confirm the chemical bonding structure between HA and PLGA. The chemical structures of pure HA and PLGA-g-HA were determined by FT-IR (Figure 2A). The change in the IR spectra can be observed by monitoring intervals (a) and (b). The carbonyl band in the ester structure has a strong stretching intensity in the range of 1735-1750 cm^{-1}.[31, 32] Interval (a), which has a peak position of 1782.5 cm^{-1}, corresponds to the carbonyl region, and the absence of a peak in this region of the HA spectrum confirms that a

carbonyl bond structure does not exist on the surface of pure HA. Since the unreacted PLGA was completely removed by centrifugation after the reaction of HA and PLGA and subsequent dissolution of the product, the detected carbonyl peak in the reacted samples arose from the surface of the reacted HA. The carbonyl structure can be observed in two major locations of the reacted HA. The first results from an esterification substitution reaction (transesterification) between the OH group present on the HA surface and PLGA. As shown in Figure 2B (a), the group with the OH unit replaces the existing ester structure. This process involves nucleophilic attack of the carbonyl carbon of PLGA ($RCOOR_1$) by the incoming alkoxide of HA (R_2O-) to give a tetrahedral intermediate, which reverts to the PLGA structure or proceeds to the transesterified product ($RCOOR_2$). The existing PLGA molecules are expected to be cut off during this process, and the molecular weight will decrease as a result. The second carbonyl structure results from reaction of the repeated ester units in the polymer chain (Figure 2B (b)). The C-O bond in the ester structure exhibits two bands from 1000-1300 cm^{-1}. This ether structure appears within interval (b), which indirectly confirms the occurrence of a chemical reaction between PLGA and HA.

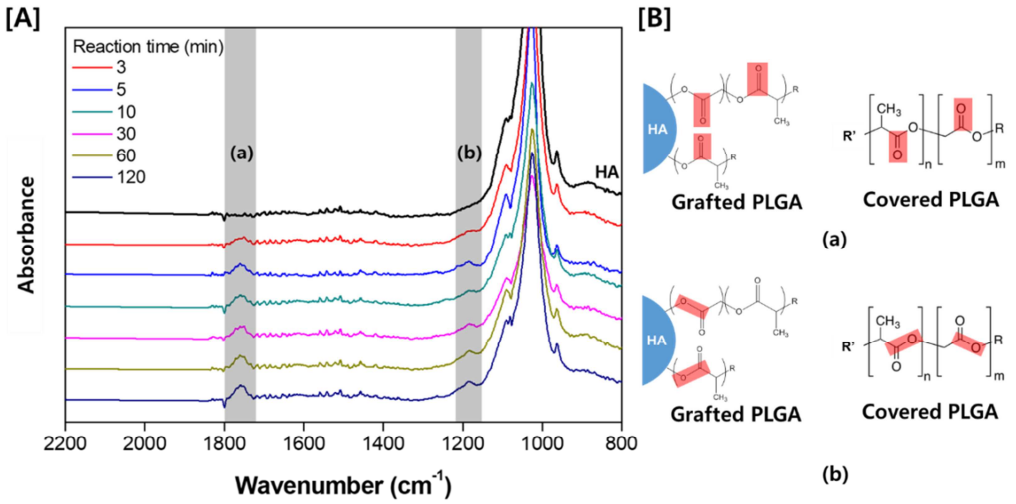

Figure 2. Results of FT-IR spectral analysis of PLGA-g-HA with a 70% HA content after various reaction times.

[A]: FT-IR spectrum and peak area for each reaction time

[B]: Main peak area analysis: (a) C=O groups with ester linkage, (b) C-O groups with ester linkage

*Grafted PLGA: Chemically bound to HA

**Covered PLGA: Physically bound to HA

Figure 3A depicts the results of ^{1}H-NMR analysis, in which changes in three regions are observed. The peak in region (a) of the spectrum of pure HA results from moisture on the surface The range from 1 to 2 ppm is the region where proton and PO_4^{3-} are bonded. As the reaction proceeds, the bound water drops off based on the broadening of the apatite PO_4^{3-} region. In the initial stage of the reaction, the area under this peak decreases, and then the peak subsequently increases as the reaction time increases. The peaks of CH and CH_2 groups appear in the range 4.5 to 5.5 ppm marked by region (a). Signals in this region correspond to the CH units in the lactic acid sites and the CH_2 units in the glycolic acid sites of PLGA. Therefore, we conclude that PLGA is continuously grafted throughout the reaction period. The peaks of CH_3 groups appear in region (b). Pure HA does not exhibit a peak in region (b), but as the reaction progresses, a new peak continuously grows. The CH_3 unit corresponds to the lactic acid structure of PLGA. Hydroxyl groups appear in region (c), and the peak observed in this region rapidly decreases as the reaction proceeds. Since the hydroxyl group is not removed in the low-temperature reaction, the observed changes confirm that this group has changed into another structure, which can be attributed to the grafting of PLGA.[33] On the other hand, the peak in the P-NMR spectrum

(Figure 3B section) does not change throughout the reaction. That is, the phosphate group is not involved in the reaction and does not undergo swelling or additional changes in the chemical structure.

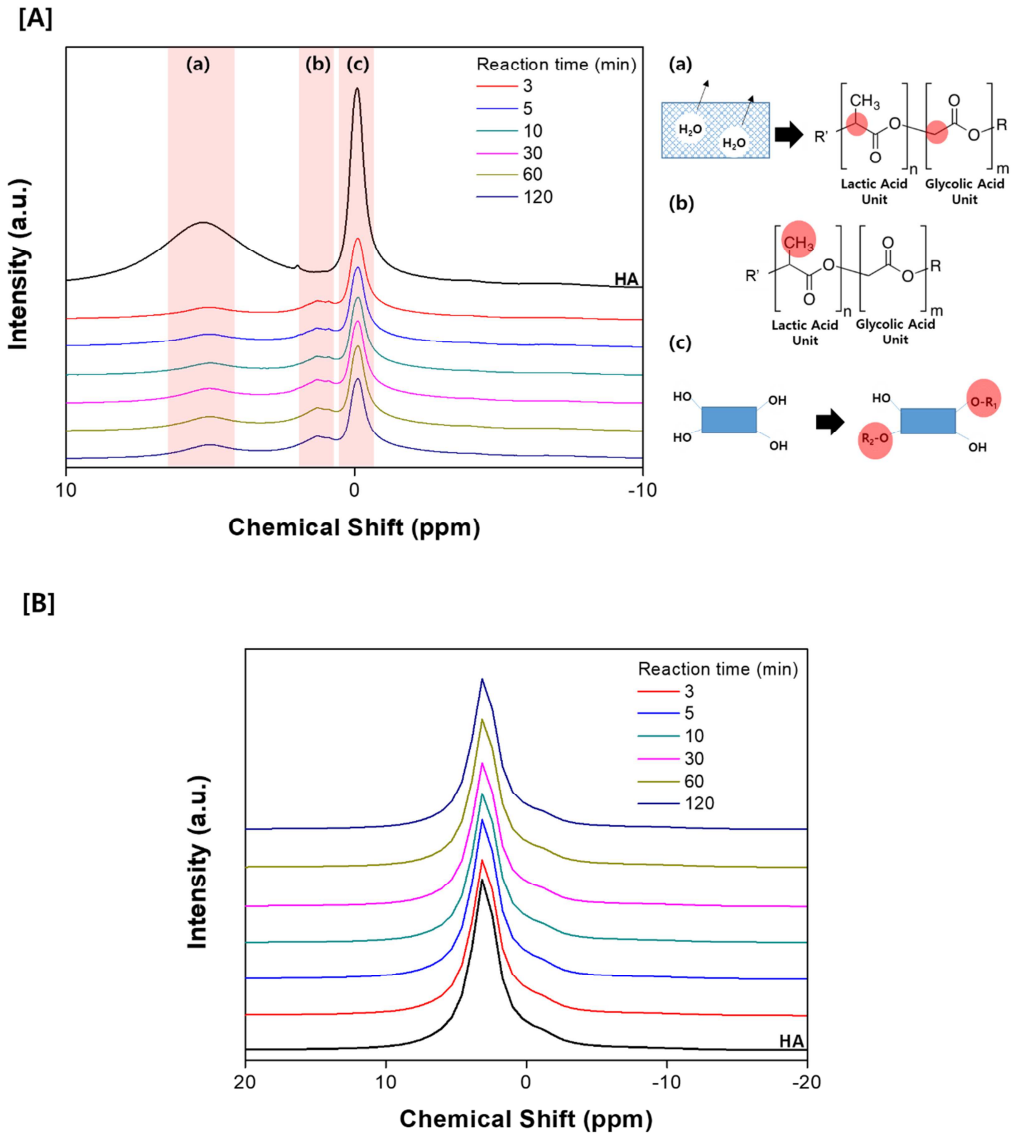

Figure 3. Solid NMR results for PLGA-g-HA with a 70% HA content after various reaction times.

[A]: ^{1}H-NMR results: (a) Peak increase due to surface H_2O desorption and increase in the number of CH and CH_2 bonds. (b) Peak increase with increasing number of CH_3 bonds. (c) Peak decrease due to OH reaction

[B]: ^{31}P-NMR results

To investigate the content of polymer grafted on the surface of HA, the products were examined by TGA. HA is an inorganic substance and therefore has a high heat resistance except for a small amount of moisture and other contaminants. The PLGA polymer structure grafted on the HA surface has a lower heat resistance than pure HA. When the temperature at which all of the polymer chains are pyrolyzed is reached during the test, all the PLGA chains that participated in the reaction are removed, and only HA is left. We thus analyzed the mass difference between samples at this temperature. To carry out these experiments, pyrolysis was performed at a temperature of 650□ or more, at which point the organic matter was completely decomposed. Bound water is eliminated from pure HA in the region from 450□ and below, and since dehydroxylation occurs above 900 □, no further mass reduction is observed in the experiment.[34] The residual weight of pure HA was estimated to be 96.3%. Figure 4 shows the results of the TGA experiments for each reaction time with an HA ratio of 70%. The weight loss observed between 400 and 450 □ is attributed to the removal of moisture from inside the HA. As the reaction time increases, the residual weight continuously decreases and then increases slightly in the 120 min reaction. As mentioned above, the difference between the residual weight of pure HA and that of the PLGA-g-HA product is related to the ratio of PLGA that was substituted on the HA surface; thus the proportion of PLGA tends to increase with increasing reaction time and then decrease in the 120 min reaction. The change in the weight at 650□

caused by grafting was calculated for various reaction times and HA contents using the following equation, and the results are shown in Figure 5 (a) and Table 1.

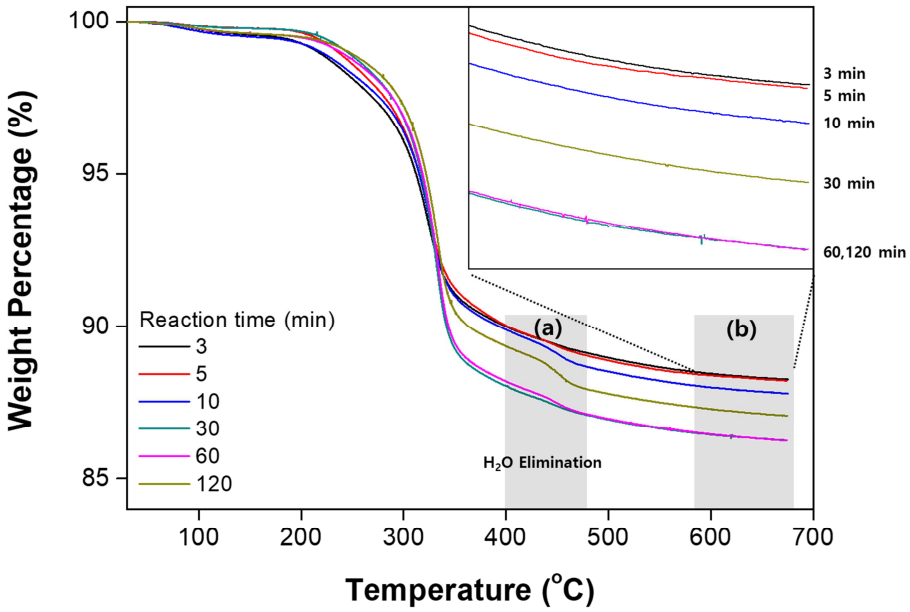

Figure 4. TGA results for PLGA-g-HA with a 70% HA content after various reaction times: (a) H_2O elimination region (b) final residue.

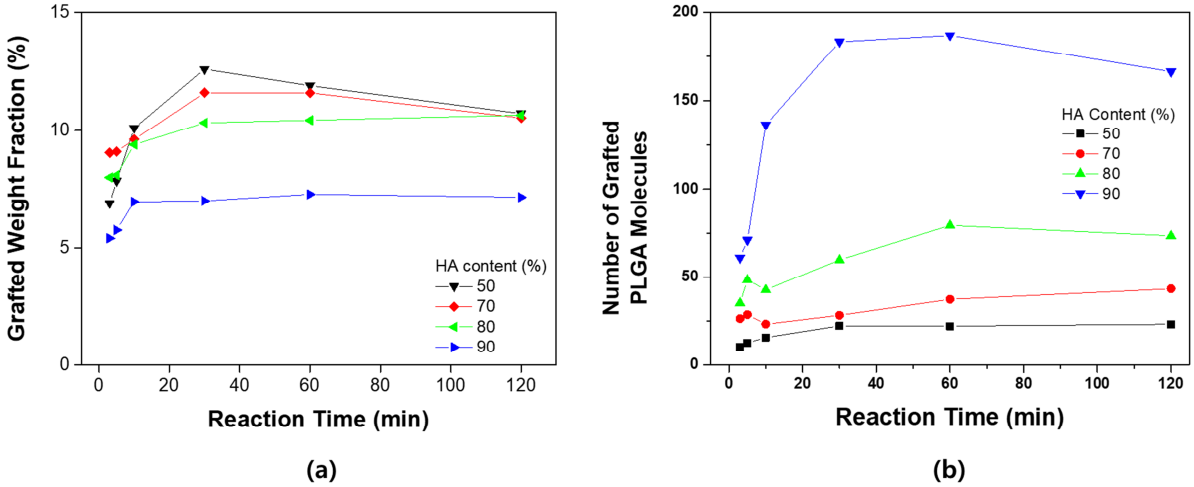

Figure 5. Results of the TGA tests for different HA contents and reaction times:

(a) PLGA residual weight ratio at 650 □. (b) Estimated number of PLGA molecules (residual weight/molecular weight) on the HA surface.

Table 1. Residual Weight of PLGA-g-HA (650□ in TGA), PLGA Weight Fraction (Calculated from the Residual Weight), and Molecular Weight (Primary Suspension) for Various HA Contents and Reaction Times.

HA Content (%)	50			70			80			90		
Reaction time (min)	Residual Weight (%)	PLGA Fraction (%)	Molecular Weight (Mw)	Residual Weight	PLGA Fraction	Molecular Weight	Residual Weight	PLGA Fraction	Molecular Weight	Residual Weight	PLGA Fraction	Molecular Weight
3	90.09	6.9%	159,929	88.30	9.1%	80,989	89.16	8.0%	53,477	91.36	5.4%	20,862
5	89.29	7.9%	148,205	88.26	9.1%	74,866	89.08	8.1%	39,485	91.06	5.8%	19,061
10	87.46	10.1%	152,283	87.85	9.6%	97,798	88.02	9.4%	51,829	90.03	7.0%	11,980
30	85.54	12.6%	133,595	86.30	11.6%	96,622	87.28	10.3%	40,668	90.00	7.0%	8,984
60	86.07	11.9%	126,754	86.30	11.6%	73,133	87.20	10.4%	30,935	89.76	7.3%	9,166
120	86.98	10.7%	108,873	87.12	10.5%	57,301	87.03	10.7%	34,118	89.86	7.2%	10,122

$$\text{Grafting weight fraction} = {Grafted\ PLGA}/{HA} = \frac{R_{HA} - R_{PHA}}{R_{PHA}}$$

In this equation, R_{HA} represents the residual weight of HA as a baseline, and R_{PHA} represents the residual weight of PLGA-g-HA. The grafting weight fraction was expected to increase proportionally with the reaction time. However, the weight fraction reaches a maximum and then decreases or remains stable. In addition, the weight fraction decreases with increasing HA content. To confirm this trend, we tested the change in the molecular weight of the PLGA dissolved in solution after the reaction of HA with PLGA by GPC. The results of the molecular weight measurements are shown in Table 1. Although the measured PLGA molecules are not directly attached to the HA surface, the results indirectly indicate that cleavage of the chains occurred and can be used to estimate the molecular weight of the PLGA attached to the HA surface. Unreacted PLGA has a molecular weight of 235K, which tends to decrease as the

reaction time with HA increases. Polymeric materials such as PLA are known to undergo continuous decomposition during thermal processing.[35, 36] The branched structure of PLA forms radicals more easily than other polymers. Therefore, cleavage of the polymer chains by radicals occurs easily. The molecular weight of PLGA also tends to decrease significantly as the HA ratio increases, and the changes in the HA content cause a greater mass loss than the changes in the reaction time. Based on the change in the molecular weight, the number of molecules that reacted under each reaction condition was calculated through the following equation.

$$\text{Grafting number fraction} = \frac{Grafting\ weight\ fraction\ (\%)}{Molecular\ weight\ (g/mol)}$$

Figure 5 (b) shows the grafting number fraction as a function of the reaction time for PLGA-g-HA samples with various HA contents. The change in the number of reaction molecules with increasing content of HA shows the opposite trend as the weight reduction; as the content of HA increases, the number of reaction molecules increases. In the pyrolysis reaction of PLGA, the surface OH groups of HA accelerate the reaction. The ability of these groups to directly participate in the substitution reaction maximizes the cleavage of the molecule. Therefore, as the HA ratio increases, the decomposition of PLGA is accelerated. When the reaction begins, the OH groups of HA react with PLGA to continuously reduce the molecular weight. Furthermore, the reaction characteristics depend on whether the ratio of PLGA or HA is dominant.

Figure 6 shows schematics of PLGA degradation and HA surface grafting for different ratios of PLGA and HA. In the PLGA-rich state shown in Figure 6A, PLGA is assumed to sufficiently cover the HA. A transesterification reaction with PLGA proceeds on the HA surface, and the section of polymer that is cut off of the chain is called the cleaved chain. The PLGA chain that is attached to the HA particle prevents another PLGA molecule from approaching the particle. This steric effect reduces the reactivity of the OH groups on the surface, and the reaction proceeds

only in the remaining space. As a result, in the case of a large amount of PLGA, PLGA chains with large molecular weights are grafted on the HA surface, and a partially unreacted hydroxyl structure remains.

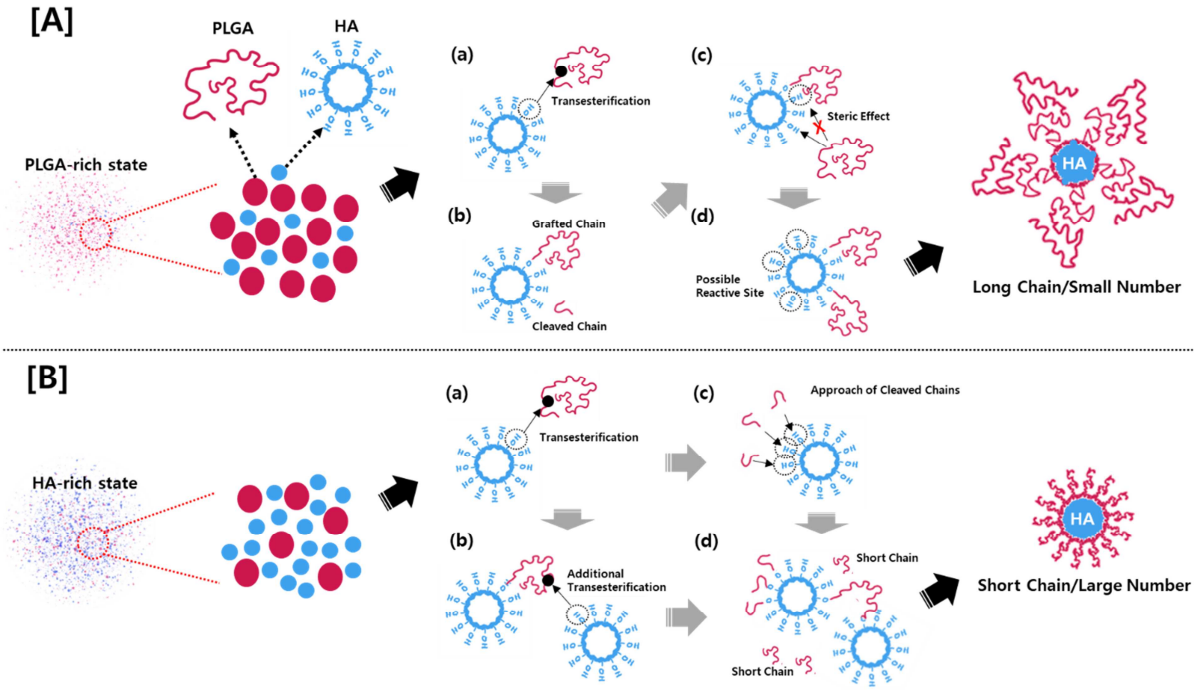

Figure 6. Analysis of the shape of PLGA-g-HA for representative PLGA/HA ratios.

[A]: PLGA-rich state: (a) Transesterification between PLGA and HA. (b) Cleaved PLGA (c) Steric effect of grafted PLGA. (d) Selective grafting of PLGA

[B]: HA-rich state: (a) Transesterification between PLGA and HA. (b) Additional transesterification between grafted PLGA and other HA particles. (c) Transesterification between cleaved PLGA and other HA particles. (d) Continuous reaction between the remaining OH groups and shortened PLGA chains

On the other hand, in the HA-rich state shown in Figure 6B, HA is capable of sufficiently reacting with PLGA, and even the PLGA chains that have already participated in the reaction

undergo additional reactions with external HA, resulting in continuous molecular weight attenuation. These phenomena lead to an increase in the amount of low-molecular-weight PLGA chains, which can participate in reactions with the remaining surface of the HA, producing a sustained response. The molecular size plays a very important role in determining the surface reactions of the materials. The smaller the molecular weight is, the easier it is for the molecule to participate in the primary reaction with the surface of HA. Therefore, when the content of HA is high, many low-molecular-weight PLGA chains are formed, and a large number of molecules react with the surface of HA.

The ratio of PLGA to HA has a large effect on the grafting number with respect to the reaction time, which can be confirmed by Figure 5 (b). For HA contents of 50% and 90%, the increase in the grafting number from the initial stage (3 minutes) to the final stage of the reaction (120 minutes) is 120% and 168%, respectively. When the HA content is high, the reaction proceeds continuously, and more molecules are grafted. As a result, it can be seen that the structural difference may occur as well as the amount of PLGA grafted on the HA surface according to the change in the ratio of PLGA and HA and the reaction time. Even if the same molecule is substituted on the surface, if the long molecule is structurally substituted, the polymer anchoring effect can be expected in the process of being used as a composite material. Therefore, mechanical strength improvement can be expected based on these condition.

We investigated the changes in the morphology of HA during the course of the grafting reaction by SEM. Figure 7A provides images showing the changes in the surface of the sample with an HA content of 70% at different reaction times. In pure HA, the particles are randomly aggregated. At the beginning of the reaction, the attachment of molecules to the surface of HA is confirmed, and at the same time, the stacking of particles thicker than the conventional HA

particles is observed. Large clusters are also distributed on the surface. This stacked structure is interpreted as the planar PLGA-g-HA structure formed by the reaction of the hydroxyl groups at the corners of the HA crystals and the PLGA.[37] Large clusters are also distributed on the surface. As the reaction progresses, the amount of these aggregated structures decreases, and a cleaner structure is formed. This trend is consistent with the increase in the particle content. The higher the particle content is, the smaller the aggregate structure surrounding HA and the more uniform the stacking. In addition, since the surface-treated HA weakens its self-aggregation property, it can be said that the dispersing property is enhanced in the process of making a composite material. Previous research on bio-composites using inorganic materials has continuously reported that the morphology changes according to the content or condition, and that such changes affect the product characteristics. [38, 39].

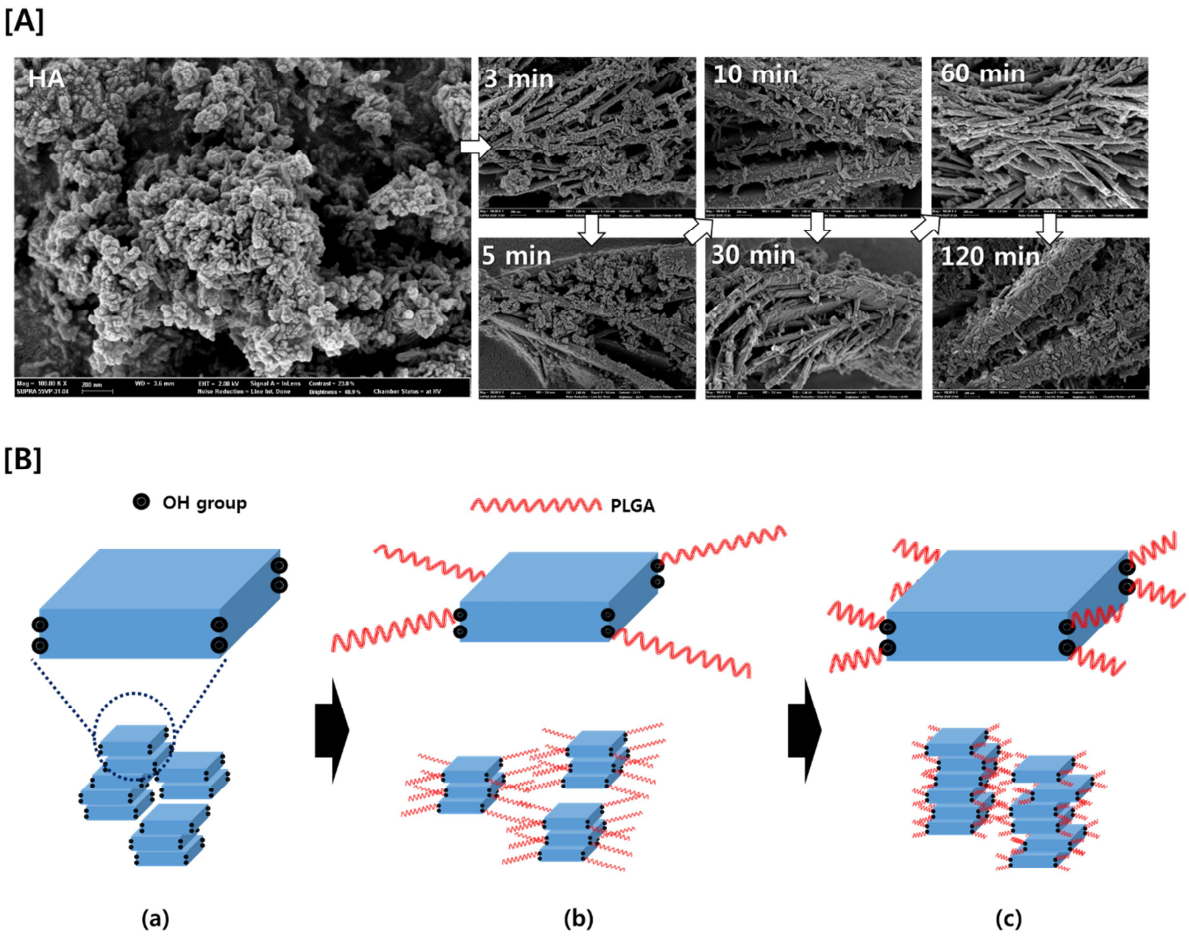

Figure 7. Evaluation of the surface of PLGA-g-HA with a 70% HA content after various reaction times.

[A]: Evaluation of the surface change at each reaction time

[B]: Schematic of the change in the aggregated structure during the reaction of HA: a) Pure HA stacking. b) Few grafted long chains on the corners of HA. C) Fully grafted short chains on the corners of HA

This change in the HA morphology is caused by the aforementioned grafting reaction and the change in the grafted PLGA molecular weight. Figure 7B shows a scheme of this process. Figure 7B (a) corresponds to the pre-reaction stage in which HA aggregates as particles. When the

reaction starts, PLGA is grafted to a portion of the HA surface. During this process, the PLGA chains have a large molecular weight and form a wide plate-like stacked structure (Figure 7B (b)). When the reaction continues, the grafting fraction of PLGA increases, as shown in Figure 7B (c), but the total molecular weight tends to decrease. Thus, the surface becomes more uniform, and the molecules on the surface form smaller clusters.

To confirm whether this structure results from crystallization, we monitored the change in the XRD peaks at various reaction times. The peaks of pure HA do not change at all throughout the reaction (Figure 8). Thus, this stacking structure can be attributed to amorphous PLGA surrounding the HA. As the content of HA increases, the reduction in the molecular weight of PLGA and the decrease in the grafting fraction can be interpreted as the formation of more homogeneous HA particles and, consequently, a change in the stacking shape. From the result of decreasing only the height without changing the shape of the peak, we can confirm again that the change of SEM image with time (Figure 7) is not the change of the stack structure of HA but the change of the structure of PLGA

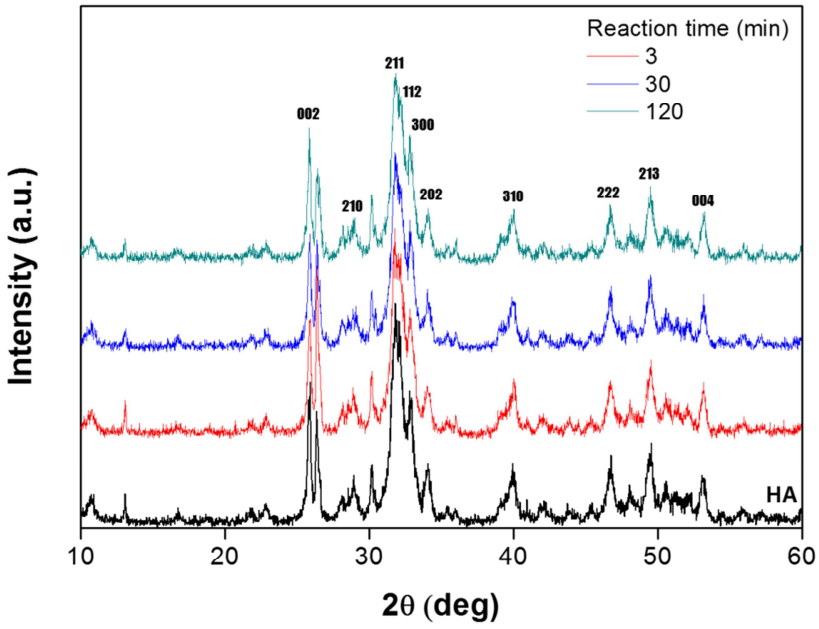

Figure 8. Analysis of the crystal structure of PLGA-g-HA with a 70% HA content at various reaction times by XRD.

DSC measurements showed that the thermal properties of PLGA-g-HA changed throughout the course of the reaction. Figure 9A shows the results of the DSC measurement of neat PLGA. Part (a) of the figure corresponds to the T_g and Tm of PLGA in the 1st scan. A T_g value of approximately 53.5 was determined from the 2nd scan shown in part (b). First, crystallization of PLGA clearly does not occur. The lactic acid region could crystallize, but the interruption by the glycolic acid region makes crystallization more difficult.[40, 41] The crystallization properties of the component materials tend to be quite different when composite materials are produced.

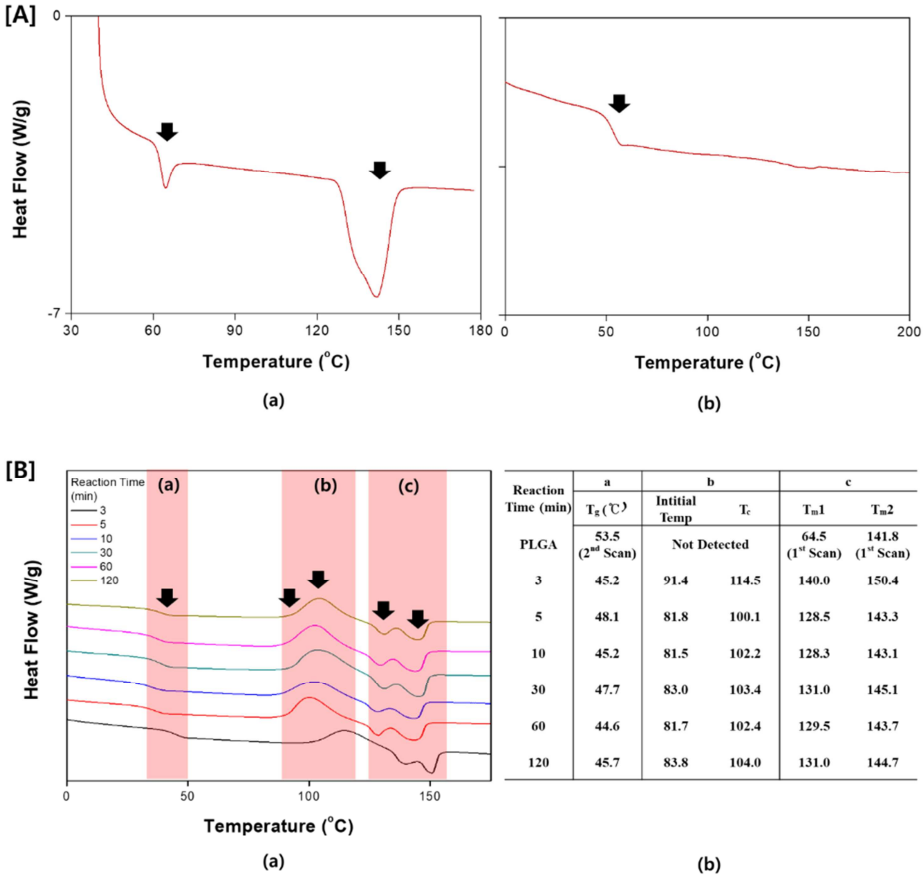

Reaction Time (min)	a	b		c	
	T_g (℃)	Intitial Temp	T_c	T_{m1}	T_{m2}
PLGA	53.5 (2nd Scan)	Not Detected		64.5 (1st Scan)	141.8 (1st Scan)
3	45.2	91.4	114.5	140.0	150.4
5	48.1	81.8	100.1	128.5	143.3
10	45.2	81.5	102.2	128.3	143.1
30	47.7	83.0	103.4	131.0	145.1
60	44.6	81.7	102.4	129.5	143.7
120	45.7	83.8	104.0	131.0	144.7

Figure 9. Results of DSC measurements of PLGA-g-HA with a 70% HA content after various reaction times.

[A]: DSC measurement results of neat PLGA: (a) 1st scan. (b) 2nd scan

[B]: DSC measurement results of PLGA-g-HA: (a) 2nd scan. (b) Analysis of the major peaks

Figure 9B section shows the DSC results of the composites prepared from PLGA-g-HA and an HA content of 70%. Although PLGA is strongly bound to the HA surface, it exhibits similar behavior to that of a general PLGA polymer. It can be assumed that PLGA is grafted as it is as a polymer phase. First, in region (a), a reduction in T_g compared with that of conventional PLGA can be confirmed. The largest decrease in T_g occurs at the beginning of the reaction, which is

influenced by the fact that the largest initial molecular weight reduction occurs at this point. As the initial molecular weight continues to decrease, T_g decreases because the mobility between molecules increases. Two major causes of this phenomenon are proposed. The first is the decrease in the molecular weight caused by the thermal degradation of PLGA that occurs when the composite material is produced. A reduction in the T_g value of a polymer caused by a decrease in the molecular weight has been previously described in the polyester research on PLLA and similar polymers. The second cause is the occurrence of transesterification by HA and the corresponding reduction in the molecular weight. A further reduction in the molecular weight could occur as a result of thermal degradation. However, since the PLGA chains are already grafted on the HA surface, the effect of thermal degradation is not expected to be large.

As heating of the composite material progresses, cold crystallization starts at an exothermic peak of 80 °C or higher. The crystallization temperature of the PLGA-g-HA formed at the beginning of the reaction is high, as PLGA is generally a non-crystalline polymer. Section A confirms that although the fraction of lactic acid is high and may be partially crystalline, it does not undergo marked crystallization. PLGA-g-HA plays a role in crystal formation in which HA acts as the nucleus. The degraded polymer block can be expected to be predominantly lactic due to the steric effects of this portion, and the resulting monomolecular polymer is expected to form crystals. In addition, a double melting phenomenon is observed, which can be interpreted as a reflection of the influence of the decomposed polymers. The melting behavior of the low-molecular-weight PLGA and of the crystalline structure formed previously affect the double melting phenomenon.

The indicators of bio-screw performance are pull-out strength and torsional strength. However, the performance is difficult to use as a relative comparative indicator because it is affected by the

injection process to manufacture the bio-screw and affected by bone condition or suture. Therefore, the results of tensile testing are the most important indicators of the applicability of PLGA-g-HA as a bio-screw. Thus, we investigated the effect of grafting PLGA on the HA surface by evaluating the tensile strength. For this experiment, composites were prepared from PLGA-g-HA with varying conditions of HA (4 types of pre-dispersion system) and a fixed reaction time of 30 min. Finally, the proportion of HA in the composite is all the same. In view of the results of the clinical application of the existing PLGA composite material, when the filler was used about 25 ~ 30%, the stability and bone regeneration characteristics of the material reached the appropriate level at the same time. Therefore, this study designed the final content of HA to be 30% [42]. Figure 10A shows the results of the tensile strength tests of neat PLGA, the blended PLGA/HA system and the composite prepared from the PLGA-g-HA master batch. All three systems have the same pure HA ratio of 30%. The simple blended PLGA/HA system exhibits a sharp, approximately 3-fold decrease in the strength compared to that of neat PLGA. On the other hand, PLGA-g-HA shows very good strength compared with that of the PLGA/HA blended system. The specimens with an HA content of 50% in the pre-dispersion process (PRE (50)) show an increase in strength of more than 100% compared with that of the PLGA/HA blended system. Comparison of the modulus of elasticity does not reveal a large overall change. However, the modulus of PRE (50) is considerably higher than that of neat PLGA. Furthermore, the elongation ratios of both the blended system and the PLGA-g-HA system both decrease dramatically relative to that of neat PLGA. Existing studies report that the mechanical strength changes with or without surface treatment. These studies basically use fibrous materials or materials with high aspect ratios. In this case, the surface modification can enhance the dispersibility and bonding properties can be expected to have the physical properties of the filler

itself. On the other hand, this study makes a difference from previous studies because it uses particulate matter. [43, 44]

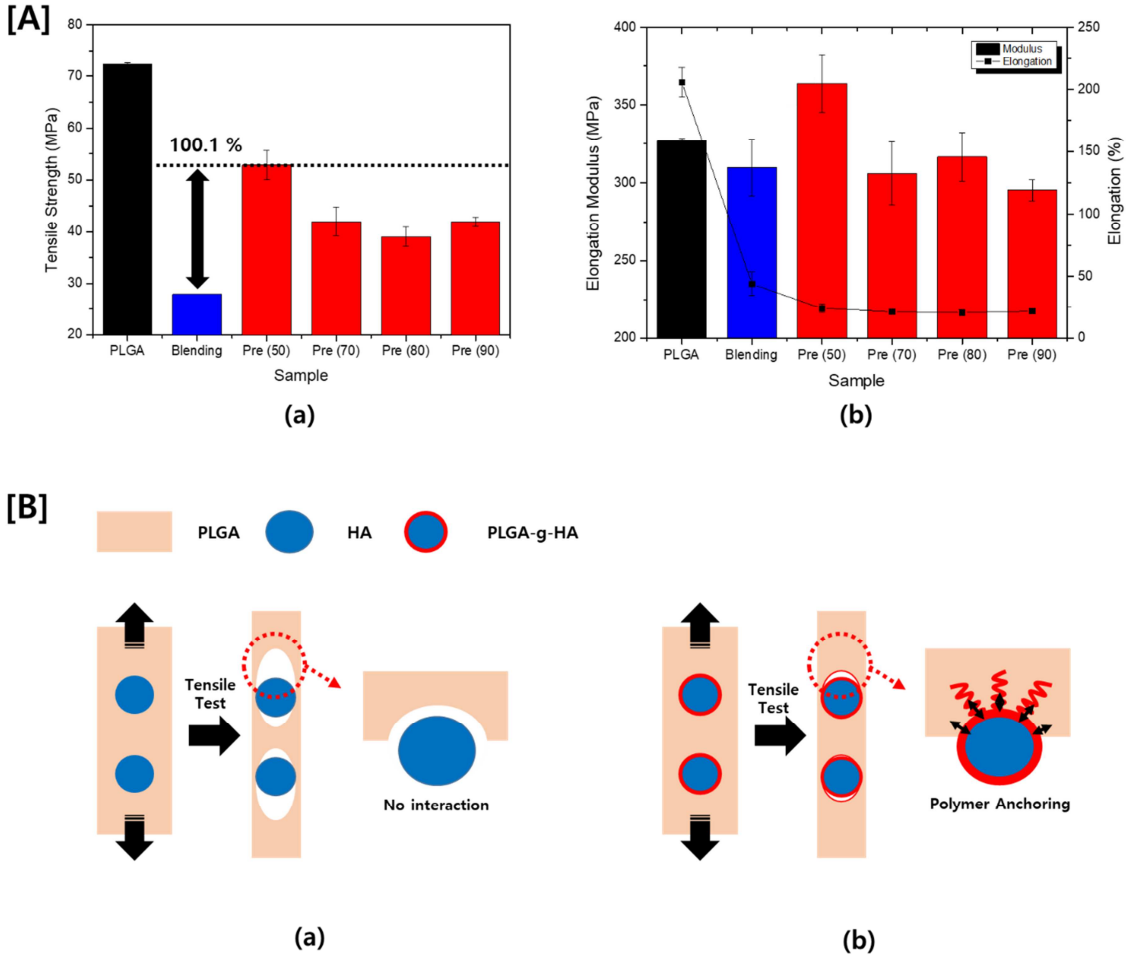

Figure 10. Evaluation of the tensile strength of the composites using PLGA-g-HA with various HA contents

[A]: Tensile strength measurement results: (a) Tensile strength. (b) Tensile modulus and elongation

(Black - neat PLGA, Blue - Simple blended specimen, Red - PLGA-g-HA composites)

[B]: Schematic diagram of the interactions in the tensile strength evaluation of the simple blended specimen and the PLGA-g-HA composites: (a) Simple blended specimen. (b) PLGA-g-HA composites

Figure 10B is a schematic diagram that illustrates the difference in the tensile strength between the blended system and the PLGA-g-HA system. Because HA is not directly associated with PLGA in the first system, it acts like a foreign substance inside the PLGA, and HA and PLGA cannot interact with each other during the tensile test. This mixed structure reduces the PLGA cross-section in the composite and simultaneously acts as a crack initiation point. On the other hand, the surface of PLGA-g-HA interacts homogenously with the PLGA matrix. The PLGA chains grafted on the HA surface diffuse into the PLGA matrix, forming anchor points between the diffused PLGA and the matrix. This effect is influenced by the molecular length of the PLGA chains grafted on the surface.[45] Therefore, the PRE (50) specimen prepared from the master batch having a 50% HA content, which is expected to have the longest molecular chains based on the results of TGA analysis, exhibits the best properties. Additionally, the elastic modulus increases to a relatively high value as a result of the anchoring effect between the PLGA matrix and HA. On the other hand, the decrease in the elongation ratio can be interpreted as a decrease in the physical properties, which is a typical consequence of using a particulate filler, as the particles interfere with the alignment of the polymer after the yield point of polymer elongation, resulting in crack initiation. As a result, it can be said that the structure has a greater influence on the mechanical performance of the composite material than the content of the substituted substance on the inorganic surface. It is important to substitute high molecular weight materials to allow physical anchoring.

The change in the mechanical properties caused by the molecular weight reduction and grafting was analyzed by DMA, and the change in the crystallization characteristics was also analyzed. Figure 11 shows the storage modulus and loss factor (tan D) of the composite systems determined via DMA. The room temperature modulus is the lowest for the sample having the highest HA content. Since the size of the grafted molecule is small and the length of the chain is short in this sample, the binding force with the PLGA matrix is expected to be low. On the other hand, when the content of HA is low, relatively long molecules are formed on the surface, and when these molecules bind with PLGA, the high modulus of HA is reflected in the results. This change is produced by the same influence of the length of the grafted PLGA chains used to describe the tensile test results.

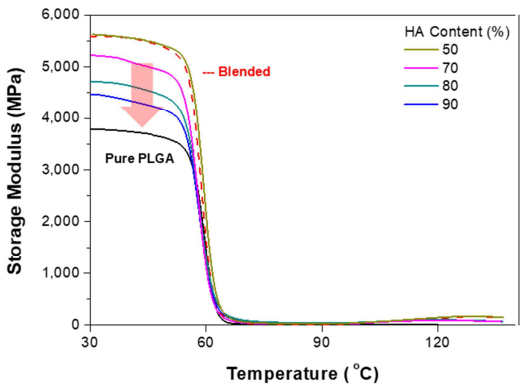

(a)

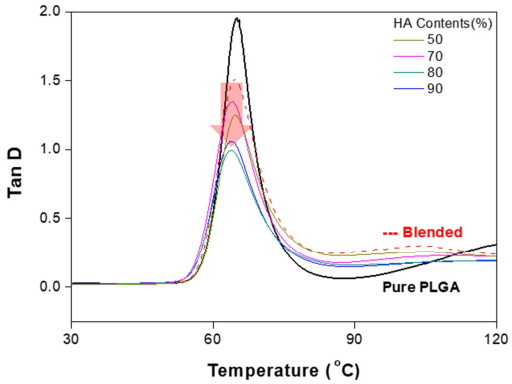

(b)

	T_g (°C)	Damping Ratio (peak)
PLGA	**65.07**	**1.95**
Blending	**64.72**	**1.51**
Pre 50	64.59	1.24
Pre 70	63.67	1.35
Pre 80	63.68	0.99
Pre 90	64.03	1.05

(c)

Figure 11. DMA measurements of the composite prepared from PLGA-g-HA having various HA contents: (a) Storage modulus focused at room temperature. (b) Loss factor (tan D). (c) Analysis of the major peak.

In the tan D evaluation, the peak tends to decrease as the HA content increases. The tan D peak represents the damping ratio of the material, which means that as the value decreases, the energy absorption characteristic becomes weaker, and the material becomes increasingly hard. As the content of HA increases, the energy absorbed by the entire material tends to decrease. This phenomenon can be attributed to two causes. First, as the molecular weight decreases, the length of the energy transfers routes inside the material decreases. In addition, the brittle characteristics introduced by the high modulus of the ceramic-based composite material also contribute.

4. CONCLUSION

The new PLGA-g-HA structure was prepared using a melt reaction method. The thermal reaction time and content of HA in the preparation of PLGA-g-HA were found to have a strong influence on the shape of PLGA-g-HA. As the reaction time increased, the number of reactive molecules on the surface increased, and the molecular length continuously decreased. As the HA content increased, the number of reactive molecules on the surface increased, while the molecular weight decreased. The molecular length of the grafted PLGA had a large effect on the performance of the composite material prepared from PLGA-g-HA. The longer the molecular length was, the stronger the interaction of PLGA-g-HA with matrix. The use of PLGA-g-HA increased the strength to more than twice that of the existing blended system. Through this method, the grafting efficiency was higher than that of the existing research, and the mechanical strength was improved at the same time. Based on these results, the applicability of PLGA-g-HA in forming PLGA composites is very high.

ACKNOWLEDGMENT

This study was supported by ARC Korea (Republic of Korea) and Seoul National University Bundang Hospital (Republic of Korea). And this work was supported by the Technology development Program (S2330276) funded by the Small and Medium Business Administration (SMBA, Korea).

REFERENCES

[1] Lo I, Griffin S, Kirkley A. The development of a disease-specific quality of life measurement tool for osteoarthritis of the shoulder: The Western Ontario Osteoarthritis of the Shoulder (WOOS) index. Osteoarthritis and cartilage. 2001;9(8):771-8.

[2] Cofield RH. Rotator cuff disease of the shoulder. JBJS. 1985;67(6):974-9.

[3] Kirkley A, Griffin S, McLintock H, Ng L. The development and evaluation of a disease-specific quality of life measurement tool for shoulder instability. The American Journal of Sports Medicine. 1998;26(6):764-72.

[4] Linsell L, Dawson J, Zondervan K, Rose P, Randall T, Fitzpatrick R, et al. Prevalence and incidence of adults consulting for shoulder conditions in UK primary care; patterns of diagnosis and referral. Rheumatology. 2005;45(2):215-21.

[5] Carr AJ, Cooper CD, Campbell MK, Rees JL, Moser J, Beard DJ, et al. Clinical effectiveness and cost-effectiveness of open and arthroscopic rotator cuff repair [the UK Rotator Cuff Surgery (UKUFF) randomised trial]. Health technology assessment. 2015.

[6] Caborn DN, Urban Jr WP, Johnson DL, Nyland J, Pienkowski D. Biomechanical comparison between Bioscrew and titanium alloy interference screws for bone—patellar tendon—bone graft fixation in anterior cruciate ligament reconstruction. Arthroscopy: The Journal of Arthroscopic & Related Surgery. 1997;13(2):229-32.

[7] Barber FA, Elrod BF, McGuire DA, Paulos LE. Preliminary results of an absorbable interference screw. Arthroscopy. 1995;11(5):537-48.

[8] Lafosse L, Brozska R, Toussaint B, Gobezie R. The outcome and structural integrity of arthroscopic rotator cuff repair with use of the double-row suture anchor technique. JBJS. 2007;89(7):1533-41.

[9] Burkhart SS, Danaceau SM, Pearce CE. Arthroscopic rotator cuff repair: analysis of results by tear size and by repair technique—margin convergence versus direct tendon-to-bone repair. Arthroscopy. 2001;17(9):905-12.

[10] Kim SH, Wise BL, Zhang Y, Szabo RM. Increasing incidence of shoulder arthroplasty in the United States. JBJS. 2011;93(24):2249-54.

[11] Kunduru KR, Basu A, Domb AJ. Biodegradable Polymers: Medical Applications. Encyclopedia of polymer science and technology. 2016.

[12] Bleul R, Maskos M. Polymersomes and their Biological Implications. Bio-and Bioinspired Nanomaterials. 2014.

[13] Locardi B, Pazzaglia U, Gabbi C, Profilo B. Thermal behaviour of hydroxyapatite intended for medical applications. Biomaterials. 1993;14(6):437-41.

[14] Tas AC, Korkusuz F, Timucin M, Akkas N. An investigation of the chemical synthesis and high-temperature sintering behaviour of calcium hydroxyapatite (HA) and tricalcium phosphate (TCP) bioceramics. Journal of Materials Science: Materials in Medicine. 1997;8(2):91-6.

[15] Zeng G, Chen T, Huang L, Liu M, Jiang R, Wan Q, et al. Surface modification and drug delivery applications of MoS2 nanosheets with polymers through the combination of mussel inspired chemistry and SET-LRP. Journal of the Taiwan Institute of Chemical Engineers. 2018;82:205-13.

[16] Ferreira J, Reis P, Costa J, Richardson B, Richardson M. A study of the mechanical properties on polypropylene enhanced by surface treated nanoclays. Composites Part B: Engineering. 2011;42(6):1366-72.

[17] Huang L, Yang S, Chen J, Tian J, Huang Q, Huang H, et al. A facile surface modification strategy for fabrication of fluorescent silica nanoparticles with the aggregation-induced emission dye through surface-initiated cationic ring opening polymerization. Materials Science and Engineering: C. 2019;94:270-8.

[18] Liu M, Ji J, Zhang X, Zhang X, Yang B, Deng F, et al. Self-polymerization of dopamine and polyethyleneimine: novel fluorescent organic nanoprobes for biological imaging applications. Journal of Materials Chemistry B. 2015;3(17):3476-82.

[19] Qiu X, Hong Z, Hu J, Chen L, Chen X, Jing X. Hydroxyapatite surface modified by L-lactic acid and its subsequent grafting polymerization of L-lactide. Biomacromolecules. 2005;6(3):1193-9.

[20] Rasal RM, Janorkar AV, Hirt DE. Poly (lactic acid) modifications. Progress in polymer science. 2010;35(3):338-56.

[21] Lee JB, Kim JE, Balikov DA, Bae MS, Heo DN, Lee D, et al. Poly (l□Lactic Acid)/Gelatin Fibrous Scaffold Loaded with Simvastatin/Beta□Cyclodextrin□Modified Hydroxyapatite Inclusion Complex for Bone Tissue Regeneration. Macromolecular bioscience. 2016;16(7):1027-38.

[22] Zhang P, Hong Z, Yu T, Chen X, Jing X. In vivo mineralization and osteogenesis of nanocomposite scaffold of poly (lactide-co-glycolide) and hydroxyapatite surface-grafted with poly (L-lactide). Biomaterials. 2009;30(1):58-70.

[23] Hu Y, Gu X, Yang Y, Huang J, Hu M, Chen W, et al. Facile fabrication of poly (l-lactic acid)-grafted hydroxyapatite/poly (lactic-co-glycolic acid) scaffolds by pickering high internal phase emulsion templates. ACS applied materials & interfaces. 2014;6(19):17166-75.

[24] Song L, Sun L, Jiang N, Gan Z. Structural control and hemostatic properties of porous microspheres fabricated by hydroxyapatite-graft-poly(D,L-lactide) nanocomposites. Composites Science and Technology. 2016;134:234-41.

[25] Cui Y, Liu Y, Cui Y, Jing X, Zhang P, Chen X. The nanocomposite scaffold of poly (lactide-co-glycolide) and hydroxyapatite surface-grafted with L-lactic acid oligomer for bone repair. Acta biomaterialia. 2009;5(7):2680-92.

[26] Jiang L, Jiang L, Xiong C, Su S. Improving the degradation behavior and in vitro biological property of nano-hydroxyapatite surface-grafted with the assist of citric acid. Colloids and Surfaces B: Biointerfaces. 2016;146:228-34.

[27] Jagur□Grodzinski J. Polymers for tissue engineering, medical devices, and regenerative medicine. Concise general review of recent studies. Polymers for advanced technologies. 2006;17(6):395-418.

[28] Kenley RA, Lee MO, Mahoney TR, Sanders LM. Poly (lactide-co-glycolide) decomposition kinetics in vivo and in vitro. Macromolecules. 1987;20(10):2398-403.

[29] Gentile P, Chiono V, Carmagnola I, Hatton PV. An overview of poly (lactic-co-glycolic) acid (PLGA)-based biomaterials for bone tissue engineering. International journal of molecular sciences. 2014;15(3):3640-59.

[30] Lan P, Zhang Y, Gao Q, Shao H, Hu X. Studies on the synthesis and thermal properties of copoly (L□lactic acid/glycolic acid) by direct melt polycondensation. Journal of applied polymer science. 2004;92(4):2163-8.

[31] Cohn D, Younes H. Biodegradable PEO/PLA block copolymers. Journal of Biomedical Materials Research Part A. 1988;22(11):993-1009.

[32] Silverstein RM, Webster FX, Kiemle DJ, Bryce DL. Spectrometric identification of organic compounds: John wiley & sons; 2014.

[33] Pereira ED, Cerruti R, Fernandes E, Peña L, Saez V, Pinto JC, et al. Influence of PLGA and PLGA-PEG on the dissolution profile of oxaliplatin. Polímeros. 2016;26(2):137-43.

[34] Tonsuaadu K, Gross KA, Plūduma L, Veiderma M. A review on the thermal stability of calcium apatites. Journal of thermal analysis and calorimetry. 2012;110(2):647-59.

[35] Signori F, Coltelli M-B, Bronco S. Thermal degradation of poly (lactic acid)(PLA) and poly (butylene adipate-co-terephthalate)(PBAT) and their blends upon melt processing. Polymer degradation and stability. 2009;94(1):74-82.

[36] Gupta M, Deshmukh V. Thermal oxidative degradation of poly-lactic acid. Colloid and Polymer Science. 1982;260(5):514-7.

[37] Zilm M, Chen L, Sharma V, McDannald A, Jain M, Ramprasad R, et al. Hydroxyapatite substituted by transition metals: experiment and theory. Physical Chemistry Chemical Physics. 2016;18(24):16457-65.

[38] Kharaziha M, Fathi M, Edris H. Effects of surface modification on the mechanical and structural properties of nanofibrous poly (ε-caprolactone)/forsterite scaffold for tissue engineering applications. Materials Science and Engineering: C. 2013;33(8):4512-9.

[39] Diba M, Fathi M, Kharaziha M. Novel forsterite/polycaprolactone nanocomposite scaffold for tissue engineering applications. Materials Letters. 2011;65(12):1931-4.

[40] Makadia HK, Siegel SJ. Poly lactic-co-glycolic acid (PLGA) as biodegradable controlled drug delivery carrier. Polymers. 2011;3(3):1377-97.

[41] Schliecker G, Schmidt C, Fuchs S, Wombacher R, Kissel T. Hydrolytic degradation of poly (lactide-co-glycolide) films: effect of oligomers on degradation rate and crystallinity. International journal of pharmaceutics. 2003;266(1-2):39-49.

[42] Damodaran VB, Bhatnagar D, Murthy NS. Biomedical polymers: Synthesis and processing: Springer; 2016.

[43] Chen J, Yan N. Mechanical properties and dimensional stability of organo-nanoclay modified biofiber polymer composites. Composites Part B: Engineering. 2013;47:248-54.

[44] Park J-W, Lee T-H, Back J-H, Jang S-W, Kim H-J, Skrifvars M. Phenyl silane treatment and carding process to improve the mechanical, thermal, and water-absorption properties of regenerated cellulose lyocell/polylactic acid bio-composites. Composites Part B: Engineering. 2019;167:387-95.

[45] Zdyrko B, Iyer KS, Luzinov I. Macromolecular anchoring layers for polymer grafting: comparative study. Polymer. 2006;47(1):272-9.